Flood Prediction using Machine Learning and GIS

Michael NYOAGBE, Ghana

John AYER, Ghana

Lily Lisa YEVUGAH, Ghana

Yaw Mensah ASARE, Ghana

Key words: Floods, Flood Risk, Geographic Information Systems (GIS), Machine Learning (ML), Rainfall Runoff.

SUMMARY

The perennial annual recurrence of floods in the Greater Accra Region brings along with it destruction and loss of lives. Flooding is considered one of the most destructive natural hazards. Prediction of these events is one sure way to mitigate their effects on lives and properties. This study developed a prediction model for extreme floods using an artificial neural network and GIS to locate impacted geographic areas prone and/or impacted by flooding. It also assessed the performance of some flood models in Greater Accra Region. A Machine Learning method (Long Short-Term Memory (LSTM)) and Geographic Information System with the application of an Analytic Hierarchy Process (AHP) relying on multicriteria method were applied considering factors such as distance to a river, Land Use Land Cover (LULC), lithology, drainage density, soil classes, rainfall, elevation, slope, and rainfall-runoff modelling were combined to predict floods within the study area. Historical floods were mapped to validate the results of the model. The results of the model showed high accuracy in predicting flash floods and demonstrate that the locations where floods would occur could be geospatially indicated to an accuracy of 80%. It further indicated the various risk zones (Very high, high, medium, and low) to flooding. The rainfall prediction gave a correlation figure of 0.953 which was considered a good correlation between the prediction model and hence made the early warning system very sensitive. The model could be improved for the prediction of floods by considering shorter rainfall periods and data from more rainfall stations.

1. INTRODUCTION

Flood is the most common natural hazard, accounting for 41% of all-natural disasters that happened globally in the last decade (CRED, 2015). There were around 1,566 floods worldwide from 2009 to 2019, affecting 754 million people and resulting in about 51,002 deaths and $371.8 billion in damage (EM-DAT, 2019). These statistics only contain "reported" instances of large-scale floods, sometimes known as flood catastrophes, in the given context. If data, recorded by the international disaster database (EM-DAT, 2019), were to include other numerous small-scale floods in which fewer than ten people died, the worldwide impact of floods would be even more catastrophic. Governments are nonetheless under pressure to deliver trustworthy and accurate flood risk maps and to develop long-term flood risk management strategies that focus on forecasting, preventing, protecting, and being prepared (CRED, 2015).

The Greater Accra Metropolitan Area in Ghana usually faces seasonal floods. The heavy rainfall mostly in the months of the May to July, Accra's low elevation, the soil's similarity to clay, inadequate and undersized drains, the dumping of trash into drains and water bodies, and the development of wetlands are the primary causes of flooding in the city. (Twumasi & Asomani-Boateng, 2002). Urban flooding, which regularly happens and results in the destruction of property and lives, has recently emerged as one of the world's issues (Kwang & Osei, 2017). Forecast uncertainty and lead time are two main issues hindering accurate flood forecasting (Liu et al., 2022). Due to climate change, it is becoming increasingly challenging to predict floods and this is leading to the destruction of lots of property, human lives and livestock.

Flood prediction models are essential for controlling extreme occurrences and evaluating risks. For the sake of future evacuation planning, policy analysis, and water resource management techniques, insightful and trustworthy projections are crucial (Mosavi et al., 2018). Improved methods for forecasting short and long-term floods as well as other hydrological events are prioritized in order to reduce damage. Forecasting floods by time and place is exceedingly challenging due to the dynamic nature of climatic variables. To replicate the intricate mathematical formulations of physical processes and basin dynamics, the most significant flood prediction models in recent years have become more data-specific and include a range of simplified assumptions (Arshad et al., 2019). These models benefit from certain techniques, such as event-driven, empirical black box, lumped and distributed, stochastic, deterministic, continuous, and hybrids (Arshad et al., 2019).

Physical models have proven to be effective at predicting a wide range of flooding situations, but they typically call for various hydro-geomorphological monitoring data, necessitating extensive calculation, and preventing short-term prediction (Mosavi et al., 2018). Due to systematic mistakes, deterministic computations are no longer accurate (Pan et al., 2018). However, recent reports indicate significant advancements in physically based flood models through model hybridization and sophisticated flow simulations (Ko & Kwak, 2012). As a result of statistical and physically based models, sophisticated data-driven techniques like machine learning, are being employed more. Machine learning (ML) is a subfield of Artificial Intelligence (AI) that uses intuitive training to understand patterns in a dataset as part of an algorithmic and heuristic approach (Arshad et al., 2019).

Although various studies have been carried out to model flooding in the Greater Accra Region using GIS, digital elevation model (DEM), and satellite-based approaches (Addae, 2018; Konadu & Fosu, 2009; Twumasi & Asomani-Boateng, 2002), it is acknowledged that methods of using ML for predicting floods in Ghana could yield improved results (Almoradie et al., 2020; Nti et al., 2021). This study aims to develop a prediction model for extreme floods using an artificial neural network and GIS. It will employ a hybrid model of ML and GIS to model and predict floods in The Greater Accra Region. The resulting model will predict the occurrence of floods using GIS data and an artificial neural network (Long-Short-Term Memory (LSTM)).

2. STUDY AREA

The scope of this study is the Greater Accra region of Ghana (Figure 1). The Greater Accra Region is geographically located between longitude 05^0 48' 0" N to 05^0 28' N, and latitude 00^0 24'30" W to 000 14' 0" E. The study area shares borders at the north by the Eastern Region, the east by the Volta Region, west by the Central Region and south by the Gulf of Guinea.

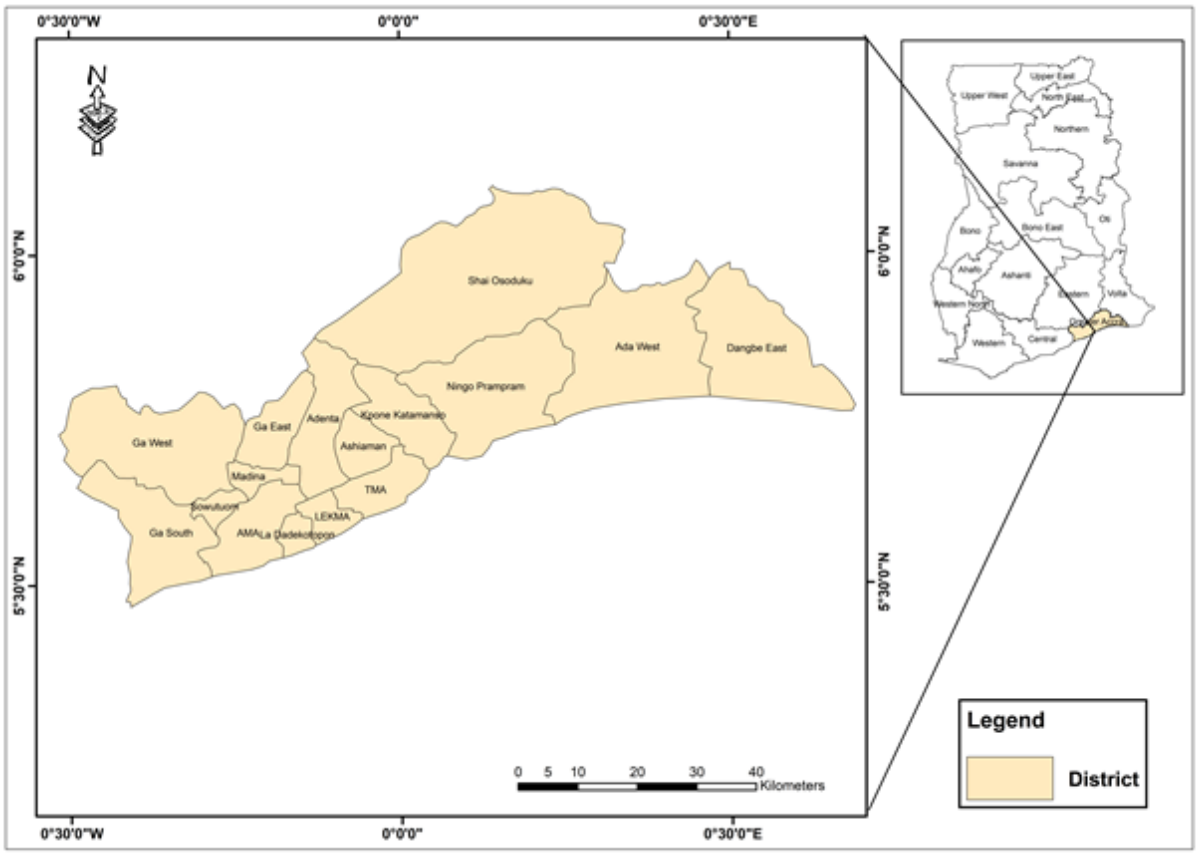

Figure 1. Map of Study Area

3.1 Data and Method

Various sources of data were considered based on their availability to develop a flood prediction model. The methodology employed was based on the flowchart indicated in Figure 2. The data used for the study are highlighted enumerated in the Table 1.

Table 1 Data sources

Item	Dataset	Source
1	Digital Elevation Model (DEM)	SRTM
2	Soil data	FAO
3	Dates and localities of flood events	NADMO
4	Rainfall, humidity, temperature, evapotranspiration	GMet, MODIS
5	River basin	Derived from DEM
6	Landuse data	Derived from Landsat8 2021 images
7	Flow rates (river basin)	Hydrological Survey Department
8	Historic Flood maps	Derived from Sentinel 1 images (2015 to 2021)
9	Lithological map	Ghana Geological Survey
10	WWF HydroSHEDS	WWF
11	JRC Global Surface Water	EC JRC / Google

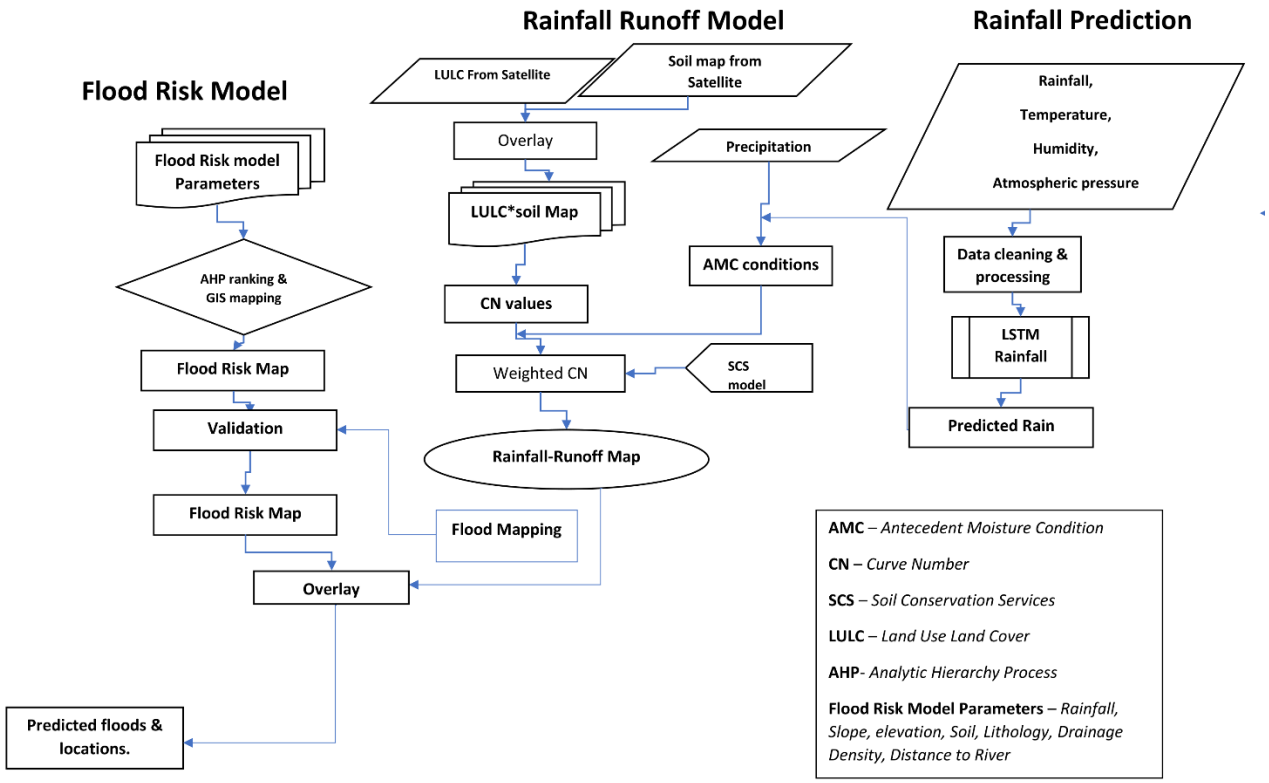

Figure 2: Flowchart on methodology

3.2 Rainfall Prediction

The input data was divided into training set (80%), test set (10%), and validation set (10%) for deep learning algorithm of LSTM to be applied for the prediction. Validation of the data was performed to provide an initial check that the model can return useful predictions in a real-world setting. The trained model was evaluated with the test set to obtain the accuracy of the prediction. Using a deep learning machine learning approach, rain was forecasted. An artificial neural network approach was used, which used input variables with environmental factors that were moderately and significantly associated to rainfall. RMSE and MAE were used to determine the performance metric.

3.2.1 Performance Assessment

Root Mean Squared Error (RMSE) and Mean Absolute Error (MAE) were used to assess the performance of the machine learning algorithm utilized in this work to forecast rainfall. Two of the most popular measures for evaluating the correctness of continuous variables were RMSE and MAE. Without considering their direction, the MAE (Equation 1) calculates the average error in a series of forecasts and the matching observation.

$MAE = \frac{1}{n}\sum_{j=1}^{n} |yj - \hat{y}|$ EA Equation 1

The average magnitude of the error was measured by the RMSE, a quadratic scoring method Shown in Equation 2 is the average of the squared discrepancies between predicted results and actual observations.

$$RMSE = \sqrt{\frac{1}{n}\sum_{j=1}^{n}(yj - \hat{y})^2} \quad \text{Equation 2}$$

Large errors are given a comparatively larger weight in RMSE. This suggests that the RMSE is most advantageous when large errors are most undesired. The variance in the errors in a set of forecasts may be identified by combining the MAE and the RMSE. The variation in the individual errors in the sample will always be bigger than the MAE or more than the RMSE, depending on how much of a difference there is between the two. All errors have the same magnitude if the RMSE = MAE.

3.3 Rainfall Run-off modelling

The rainfall-runoff model based on the Curve Number (CN) approach (Soil Conservation Service 1964; 1972) was built using Google Earth Engine (GEE). Through the JavaScript API, all the fundamental datasets— (soil, LULC, and rainfall) image data were loaded into GEE. The CN II maps were initially created by converting the soil texture map into a soil group map and combining it with Land Use Land Cover. The total amount of precipitation over the previous five days was used to determine Antecedent Moisture Condition (AMC) data. Depending on the AMC circumstances of each pixel, the daily run-off was determined. The model calculated the surface run-off based on the extent of the study area.

3.4 SCS CN model development

The classical CN technique, which is based on the water budget equation as shown in Equation 3, is an event-based, lumped rainfall-runoff model.

$$P = Ia + F + Q \quad \text{Equation 3}$$

Two proportional equality hypotheses are expressed in Equation 4 and Equation 5 as follows

$$\frac{Q}{P-Ia} = \frac{F}{S} \quad \text{Equation 4}$$

$$Ia = \lambda S \quad \text{Equation 5}$$

Where *P* represents the amount of daily precipitation, *Ia* denotes the preliminary abstraction, *F* denotes real retention, *Q* denotes direct surface run-off, S denotes prospective highest retention, and denotes the initial abstraction coefficient.

The well-known SCS CN equation is shown in Equations 6 and 7 by combining the two equations 4 and 5.

$$Q = \begin{cases} \frac{(P-Ia)^2}{P-Ia+S} & \text{for} \quad P > Ia, \\ 0 & \text{for } P \leq Ia \end{cases} \quad \text{Equation 6}$$

where *S* is a function of CN and can be computed using Equation 7.

$$S = 25.4\left(\frac{1000}{CN} - 10\right) \quad \text{Equation 7}$$

where *S* is measured in millimeters and *CN* is a dimensionless run-off coefficient that relies on the type of land used, the type of soil, and the pre-existing moisture state *(AMC).*

An important factor in the run-off process is antecedent moisture, which is the catchment's relative dryness or wetness as it varies through time. Three classifications can be used to describe AMC.

When there has been no rainfall in the previous five days, or when AMC is less than 13 mm, AMC I is taken into consideration. A moist state (AMC III) may exist when AMC is greater than 28 mm, and an average condition (AMC 28 mm) may exist (AMCII). Based on the LULC and soil group characteristics, CNs have been recommended for AMC II. In relation to AMC I and AMC III, CN (Equations 8 and 9).

$$CN(I) = \frac{CN\ (II)}{2.281 - 0.0128CN(II)} \quad \text{Equation 8}$$

$$CN(III) = \frac{CN\ (II)}{0.427 - 0.00573CN(II)} \quad \text{Equation 9}$$

[*Ponce and Hawkins*, 1996; *Rallison and Miller*, 1982; *USDA National Resources Conservation Service*, 2004]

The rainfall-runoff modeling was carried out using GEE after indicating the different input data. The ternary operator in image expression was originally used to translate the soil texture map into the four hydrologic soil groups A, B, C, and D. Then it is included as a second band in the downscaled LULC MODIS data. The conditional statement is then used to construct the curve number two (CN II) map for each combination. There are four soil groupings and MODIS LULC data classes. The CN I and CN III maps are created using CN II and Equations 6 and 7. The S image, which depends on AMC, performs the CN image's purpose. As a result, during the final Q calculation, the S pictures corresponding to CN maps are generated. The script creates S images as a global variable to speed up processing for all CN circumstances. Utilizing daily rainfall data images, daily AMC images are produced. For each day of the study period, an AMC collection was created using the five days prior, including same-day rainfall.

The S-I image calculated from CN I is used to replace pixels with an AMC of less than 13 mm, while the S-III image computed from CN III is used to replace pixels with an AMC of

than or equal to 28 mm. To create a single S picture for each day that meets the AMC criterion for all pixels, the three images are combined. If rainfall for a single pixel on a single day is less than *Ia*, the consequent run-off will be 0; otherwise, the run-off is approximated using the previously described function. This condition is then tested after using the equation for run-off computation.

To obtain the run-off images for each date, this function is mapped across the whole collection of AMC and rainfall. Both characteristics are integrated in a single image for each date to

display the graph of rainfall and runoff. The images were then aggregated together to create the sum of images of rainfall and runoff, which is then used to create the final time series graph.

3.4 Flood Risk modelling

To develop a flood risk map using the AHP method, 8 input parameters (elevation, slope, distance from river, drainage density, rainfall, LULC, soil and lithology) were used. Each of the input features were classified into sub classes. The elevation, slope, distance to river, drainage density, LULC, soil and lithology were reclassified into five classes with respect to their flood causing properties. Rainfall was classified into three classes of high, medium and low indicating the rainfall intensity for the period under consideration.

To obtain risk assessments for the evaluation of flood risk, a table questionnaire was given to various experts based on what was done by Allafta & Opp (2021). Indicated in the table are factors to consider for this study, these are eight flood influencing factors (precipitation, geology, drainage density, Digital Elevation Model, Land Use Land Cover, terrain slope, soil characteristics, and distance from river). The experts were instructed to choose one parameter (for example, precipitation) and evaluate against the other parameters one at a time to determine "*which parameter is more important*?" with regards to flooding. The experts then used their knowledge to compare the pairing of these aspects. And how significant is that in Saaty's eyes? (Harker & Vargas, 1987) and their significance on a scale of 1 to 9 are shown in Table 1.

Table 1: The factor relevance scale

level of importance	Description
1	Equal significance
3	Medium significance
5	Strong
7	Very strong significance
9	Maximum significance
2, 4, 6, and 8	Intermediate between two adjacent values

An 8x8 pairwise comparison matrix for the mapping of flood hazards (Table 2) was generated based on the excel template created by (Goepel, 2013b).

Table 2: An 8 x× 8 pairwise comparison matrix for the AHP-based flood hazard mapping

	PRf	SDR	EDEM	LSl	LULC	DD	LSo	RLt	Normalized principal Eigenvector
PRf	1	1 ½	1 1/7	2	2 1/4	1 1/2	1 7/9	2 2/3	19.57%
SDR	2/3	1	1 1/2	1 1/7	2	1 1/4	1 2/3	2 1/2	16.06%
EDEM	7/8	2/3	1	1	1 1/2	1 1/6	1 5/9	3	14.20%
LSl	½	7/8	1	1	1 1/2	1 3/4	1 4/9	2 1/2	13.99%
LULC	4/9	½	2/3	2/3	1	1 3/4	1 4/9	2 1/6	11.07%
DD	2/3	4/5	6/7	4/7	4/7	1	1 1/3	2	10.57%
LSo	4/7	3/5	2/3	2/3	2/3	3/4	1	1 1/2	8.89%

RLt	3/8	2/5	1/3	2/5	1/2	1/2	2/3	1	5.65%
Sum	**5**	**6 1/3**	**7 1/7**	**7 1/2**	**10**	**9 2/3**	**10 8/9**	**17 1/3**	**100.00%**

The principal eigenvalue (λmax) indicates the matrix deviation from consistency (Brunelli & Fedrizzi, 2013). A pairwise matrix was considered to be consistent only when the λmax is equal or higher than the number of the parameters investigated; or else, a new matrix should be generated (Allafta & Opp, 2021b). The principal eigen-value λmax in Table 3 was achieved by the summation of products of the sum of parameter columns in the pairwise matrix in Table 2 and the eigenvectors in Table 3. A principal ei-genvalue of 8.14 for an 8*8 matrix was achieved and applied to calculate of the consistency measure (Table 1).

Table 3: Computation of the principal Eigenvalue (λmax) to rank influence of parameter

	Column sums row 10 of Table 4 (1)	Eigenvectors column 11 of Table 4 (2)	Parameter rank (1)*(2)
PRf	5	0.196	0.98
SDR	6 1/3	0.161	1.02
EDEM	7 1/7	0.142	1.01
LSl	7 1/2	0.14	1.05
LULC	10	0.111	1.11
fDD	9 2/3	0.106	1.02
LSo	10 8/9	0.089	0.97
RLt	17 1/3	0.057	0.98
Sum (λmax)			**8.14**

Note: PRf = Rainfall; SDR = Distance to River; EDEM = Digital Elevation Model; LSl = Slope; LULC = Land Use Land Cover; fDD = Drainage Density; LSo = Soil; RLt = Lithology.

Table4: Random Index table

Number of parameters	1	2	3	4	5	6	7	8	9	10
RI	0	0	0.58	0.9	1.12	1.24	1.32	1.41	1.45	1.49

Calculating the consistency ratio, the normalized weight's consistency could be assessed (Allafta & Opp, 2021c). The given weights were only considered consistent when the consistency ratio is equal to or less than 10%; otherwise, these weights needed to be reevaluated in later rounds to minimize inconsistency (Harker & Vargas, 1987). The consistency index (CI) was calculated in order to calculate the consistency ratio according to Saaty (1988):

$$CI = \frac{\lambda max - n}{n-1} \qquad \text{Equation 10}$$

where *max* is the largest eigenvalue and n is the total number of different theme layers. The *CI* in this study is established by:

$$CI = \frac{(8.14-8)}{8-1} = 0.02$$ Equation 11

Equation 11 was used to calculate the consistency ratio (CR):

$$CR = \frac{CI}{RI}$$ Equation 12

where RI for different n parameters represents the random index provided in Table 4. In this study, RI is calculated as 1.41 based on the eight criteria considered. CR therefore equals: 0.02/1.41 = 0.014184

According to their importance in terms of flood vulnerability, weight ratings were given to the various thematic layers together with their respective classes during the study. Using the expertise of experts, weights were allocated to the layers and classes (Tables 3 and 4). The total scores were then calculated using a straightforward weighted sum. Each pixel of the resulting map (Hi) was calculated using the equation shown below (Sumit, 2018):

$$Hi = \sum_j^n Wj \times \text{Xij}$$ Equation 13

Where *Wj* denotes the *j* layer's normalized weight, and *Xij* denotes the rank scores of each class relative to the *j* layer.

The flood model was then used to access the accuracy of the flood risk model. Areas with very high risk, high risk, moderate and low risk were check for consistency with historic flood events and used to determine the accuracy of the flood risk model. Spatial overlay analysis was employed in this assessment.

4. RESULT

The output of the proposed (LSTM)-based rainfall prediction model for forecasting rainfall over a 30-day period is shown in Figure 3.

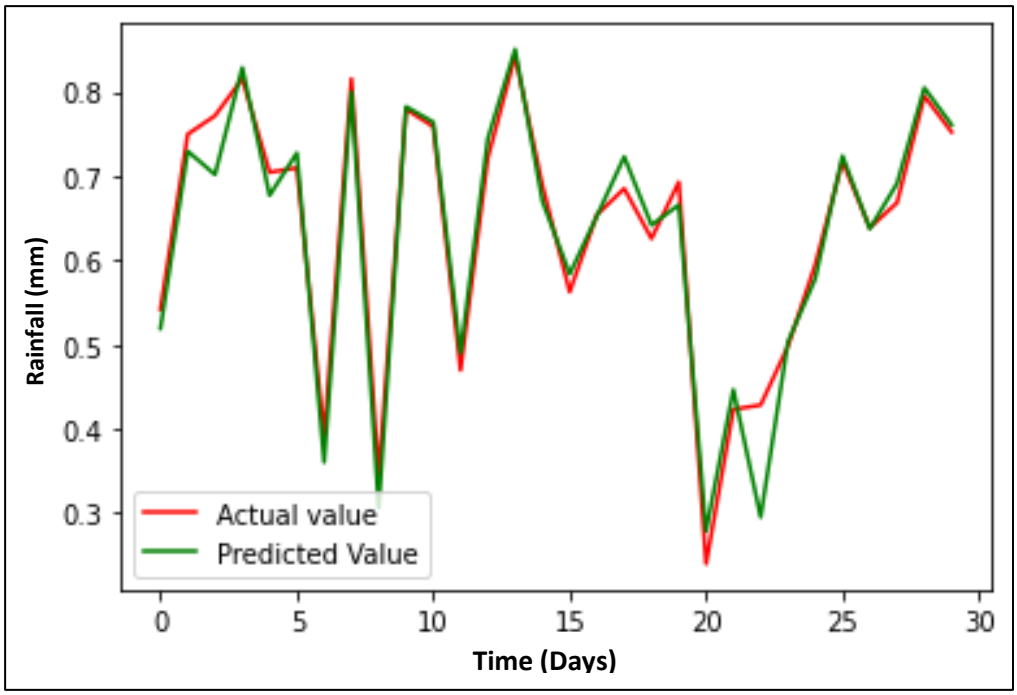

Figure3: Rainfall Prediction mode

The figure displays the Greater Accra Region's actual daily rainfall levels as determined by GMet and the 30-day rainfall forecast. The findings demonstrated that the proposed technique is 95.25% accurate in predicting average rainfall (in mm). On the graph, the green line shows the amount of average daily rainfall predicted by the model, while the red line reflects the amount of average daily rainfall observed by the rain gauge. The actual values and the forecast had a 0.953 correlation, which is a strong correlation. Consequently, it is possible to forecast rainfall for a certain day using the suggested model.

The LSTM had an RMSE of 0.0366 and an MAE of 0.0267 with and confidence level (R2%) of 95.25%. The outcomes of the implemented model were contrasted with those of earlier techniques for predicting rainfall. Although using deep learning to forecast rainfall improves accuracy, it was found that the implemented model underperformed Endalie et al. (2021) techniques by 4.47% in terms of RMSE because fewer input parameters were used due to lack of data.

Four risk classes were obtained from the analysis (Very High, High, Medium and Low). The related zones indicating the flood prediction created using the 8 parameters employed in hazard mapping are summarized in Table 5. The findings revealed four separate groups of risk (zones) within the basin that represented four values and their corresponding risk classes of flood threats.

Out of the eight variables employed in the hazard mapping, the flood forecast was created from the flood risk map. In the basin, these results led to the creation of 5 separate classifications (zones) that correspond to very high, high, medium, low, and very low flood threats (Figure 4). These zones made 0.015%, 11.48%, 13.91%, and 74.27% of the basin area of the research region, respectively.

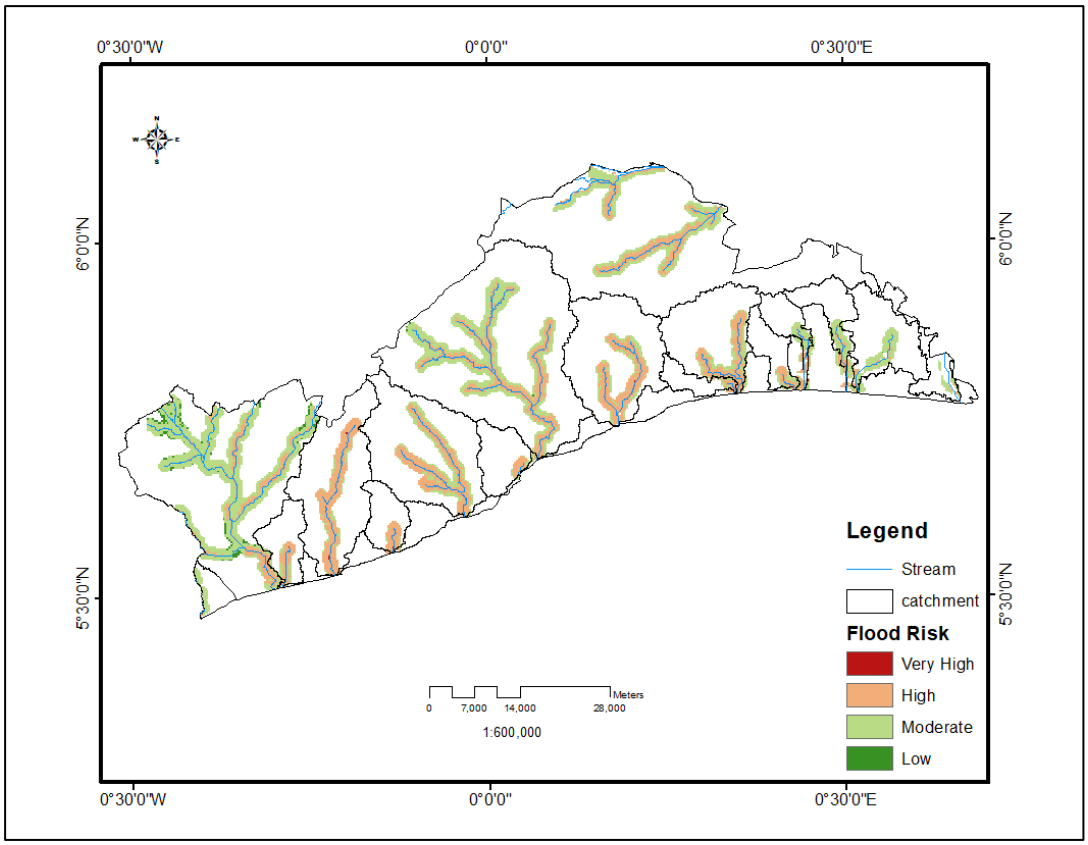

Figure 4: Flood Risk map

Table 4. Flood Risk Zones

Value	Risk Class	Area(km^2)
1	Very High	372.57
2	High	451.49
3	Medium	10.50
4	Low	372.57

Distance to river, slope, DEM, and drainage density all have a positive impact on the high and very high zones in this study. Risk to flooding and the likelihood that it will happen again are increased by being closer to rivers, living within areas of low elevations and having relatively high drainage density.

Moderate flood hazard zones are found along the rivers in those subbasins due to the influence of areas with Relatively high elevations and low drainage density, but they are farther away from the very high and high zones, which are anticipated to be produced by the highest rainfall levels in the middle to southern regions extending east and westward of the watershed (Figure 5).

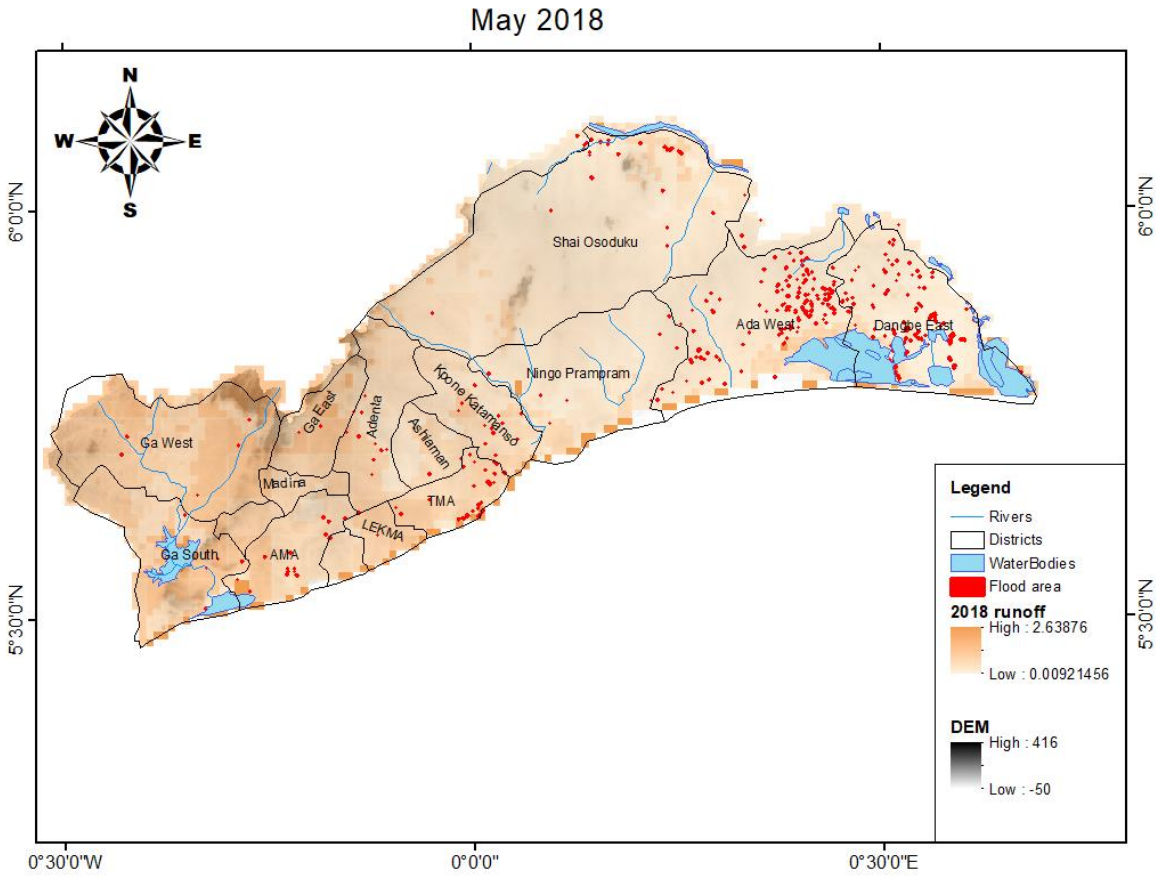

Figure 5. Runoff and Flood Mapping For 25th May 2018

In contrast, the low and very low zones are farthest from the river body and these areas have the least susceptibility to floods since they have the lowest drainage density and are farthest from the river. Within the catchment area of the study, it was found that the bulk of the places with very high- and high-risk zones were in the areas with very high and high rainfall.

5. CONCLUSION AND RECOMMENDATIONS

In conclusion, the results of flood prediction using LSTM based prediction of rain and the AHP flood risk modelling proved very effective in predicting floods in the Greater Accra Region of Ghana. The SCS curve number method of run-off modelling method in GEE transforms predicted precipitation into runoffs. This indicates the applicability of Machine Learning and GIS in flood prediction.

In predicting floods, one of the most sensitive inputs to floods is rainfall. When rainfall is predicted accurately, the other factors are physical factors such as runoff. There are several factors however that affect the amount of runoff which helps determine the intensity of flooding within an area.

To improve on the accuracy of the rainfall prediction, other parameters such as wind speed and sunshine could be considered. When much more meteorological parameters are considered, the likelihood of increasing the model's accuracy is higher.

Further studies need to be carried out to predict rainfall at shorter time intervals from the radar images and possibly GNSS CORS data. This will improve the prediction models for rainfall developed in this study which focused on the 30-day daily total rainfall.

References

Abbot, J. & Marohasy, J. (2014). Input selection and optimization for monthly rainfall forecasting in Queensland, Australia, using artificial neural networks. *Atmospheric Research, 138*, 166–178. https://doi.org/10.1016/J.ATMOSRES.2013.11.002

Adamowski, A., Chan, H. F., Prasher, S. O., Ozga-Zielinski, B., & Sliusarieva, A. (2021). *Comparison of multiple linear and nonlinear regression, autoregressive integrated moving average, artificial neural network, and wavelet artificial neural network methods for urban water demand forecasting in Montreal, Canada*. Water Resources Research. https://agupubs.onlinelibrary.wiley.com/doi/epdf/10.1029/2010WR009945

Addae, R. A. (2018). Satellite-Based Flood Mapping for Hydrodynamic Flood Model Assessment: Accra, Ghana (Masters' thesis). *Masters' Thesis*.

Addei, I. (2016). *Causes and effects of perennial flooding in urban centres in Ghana - Graphic Online*. Graphic Communications Group Limited. https://www.graphic.com.gh/features/opinion/causes-and-effects-of-perennial-flooding-in-urban-centres-in-ghana.html

Ahamed, N., & Asha, S. (2020). Flood prediction forecasting using machine Learning Algorithms. *International Journal of Scientific & Engineering Research, 11*.

Allafta, H., & Opp, C. (2021). GIS-based multi-criteria analysis for flood prone areas mapping in the trans-boundary Shatt Al-Arab basin, Iraq-Iran. *Http://Www.Tandfonline.Com/Action/JournalInformation?Show=aimsScope&journalCode=tgnh20#.VsXodSCLRhE*, *12*(1), 2087–2116. https://doi.org/10.1080/19475705.2021.1955755

Almoradie, A., de Brito, M. M., Evers, M., Bossa, A., Lumor, M., Norman, C., Yacouba, Y., & Hounkpe, J. (2020). Current flood risk management practices in Ghana: Gaps and opportunities for improving resilience. *Journal of Flood Risk Management*, *13*(4). https://doi.org/10.1111/jfr3.12664

Arshad, B., Ogie, R., Barthelemy, J., Pradhan, B., Verstaevel, N., & Perez, P. (2019a). Computer vision and iot-based sensors in flood monitoring and mapping: A systematic review. *Sensors (Switzerland)*, *19*(22). https://doi.org/10.3390/s19225012

Barrera-Animas, A. Y., Oyedele, L. O., Bilal, M., Akinosho, T. D., Delgado, J. M. D., & Akanbi, L. A. (2022a). Rainfall prediction: A comparative analysis of modern machine learning algorithms for time-series forecasting. *Machine Learning with Applications*, *7*, 100204. https://doi.org/10.1016/J.MLWA.2021.100204

Besse Rimba, A., Diah Setiawati, M., Sambah, A. B., Miura, F., & Smith, M. P. (n.d.). Physical flood vulnerability mapping applying geospatial techniques in Okazaki City, Aichi Prefecture, Japan. *Mdpi.Com*. https://doi.org/10.3390/urbansci1010007

Cabrera, J. S., & Lee, H. S. (2019). Flood-prone area assessment using GIS-based multi-criteria analysis: A case study in Davao Oriental, Philippines. *Water (Switzerland)*, *11*(11). https://doi.org/10.3390/W11112203

Costabile, P., Costanzo, C., & MacChione, F. (2013). A storm event watershed model for surface runoff based on 2D fully dynamic wave equations. *Hydrological Processes*, *27*(4), 554–569. https://doi.org/10.1002/HYP.9237

CRED. (2015). The human cost of natural disasters. In *Centre for Research on the Epidemiology of Disasters CRED*.

Das, S. (2018). Geographic information system and AHP-based flood hazard zonation of Vaitarna basin, Maharashtra, India. *Arabian Journal of Geosciences 2018 11:19*, *11*(19), 1–13. https://doi.org/10.1007/S12517-018-3933-4

EM-DAT. (2019a). *EM-DAT | The international disasters database*.

Endalie, D; Haile, G; & Taye, W. (2022). Deep learning model for daily rainfall prediction: case study of Jimma, Ethiopia. *Water Supply, 22(3), 3448-3461*.

Fawcett, R. J. B., & Stone, R. C. (2010). The seasonal forecasting systems. *Australian Meteorological and Oceanographic Journal*, *60*, 15–24.

Fox, N. I., & Wikle, C. K. (2005). A Bayesian Quantitative Precipitation Nowcast Scheme. *Weather and Forecasting*, *20*(3), 264–275. https://doi.org/10.1175/WAF845.1

Ghana Statistical Service. (2013). *2010 Population & Housing Census: Regional Analytical Report Greater Accra Region*. 134.

Goepel, K.D. (2013) Implementing the Analytic Hierarchy Process as a Standard Method for Multi-Criteria Decision Making In Corporate Enterprises—A New AHP Excel Template with Multiple Inputs. Proceedings of International Symposium on the Analytic Hierarch. International Symposium on the Analytic Hierarchy Process, Kuala Lumpur. https://www.scirp.org/reference/ReferencesPapers.aspx?ReferenceID=1979930

Harker, P. T., & Vargas, L. G. (1987). *The Theory of Ratio Scale Estimation: Saaty's Analytic Hierarchy Process on JSTOR*. Management Science Vol 33, No. 11. https://www.jstor.org/stable/2631919

Isikdogan, L. F., Bovik, A., & Passalacqua, P. (2020). Seeing through the Clouds with DeepWaterMap. *IEEE Geoscience and Remote Sensing Letters*, *17*(10),1662–1666. https://doi.org/10.1109/LGRS.2019.2953261

Kim, B., Sanders, B. F., Famiglietti, J. S., & Guinot, V. (2015). Urban flood modeling with porous shallow-water equations: A case study of model errors in the presence of anisotropic porosity. *Journal of Hydrology*, *523*, 680–692. https://doi.org/10.1016/J.JHYDROL.2015.01.059

Knightes, C. (2017). *An Overview of Rainfall-Runoff Model Types An Overview of Rainfall-Runoff Model Types*. *September*, 0–29.

Ko, B; & Kwak, S. (2012). Survey of computer vision-based natural disaster warning systems. *Optical Engineering, 51(7), 070901.*

Konadu, D. D., & Fosu, C. (2009b). Digital Elevation Models and GIS for watershed modelling and flood prediction - A case study of Accra Ghana. *Appropriate Technologies for Environmental Protection in the Developing World - Selected Papers from ERTEP 2007*, 325–332. https://doi.org/10.1007/978-1-4020-9139-1_31

Mosavi, A; Ozturk, P; & Chau, K. (2018). Flood Prediction Using Machine Learning Models:Literature Review. *Water 2018, Vol. 10, Page 1536, 10(11), 1536.*

Sumit, D. (2018). Geographic information system and AHP-based flood hazard zonation of Vaitarna basin, Maharashtra, India. *Arabian Journal of Geosciences 2018 11:19, 11(19), 1–13*.

Twumasi, Y. A; & Asomani-Boateng, R. (2002). Mapping seasonal hazards for flood management in Accra, Ghana using GIS. *IEEE international geoscience and remote sensing symposium (Vol. 5, pp. 2874-2876).*

Wang, Y., Li, Z., Tang, Z., & Zeng, G. (2011a). A GIS-Based Spatial Multi-Criteria Approach for Flood Risk Assessment in the Dongting Lake Region, Hunan, Central China. *Water Resources Management*, *25*(13), 3465–3484. https://doi.org/10.1007/S11269-011-9866-2

Zou, Q., Zhou, J., Zhou, C., Song, L., & Guo, J. (2012). Comprehensive flood risk assessment based on set pair analysis-variable fuzzy sets model and fuzzy AHP. *Stochastic Environmental Research and Risk Assessment 2012 27:2*, *27*(2), 525–546. https://doi.org/10.1007/S00477-012-0598-5

Biographical notes

Ing. Surv. Michael Nyoagbe is a Geospatialist and a Manager at the Ghana Water Company Limited at the Technology and Innovation Department where he works as a GIS Officer and Research and Development Manager. He has a career in GIS Consultancies internationally and application development. His research interest focuses on Artificial Intelligence and GIS amongst many other areas. He is the President of the Ghana Geospatial Society, a member of Ghana Institution of Engineering, Licensed Surveyors Association of Ghana, Ghana Institution of Surveyors, and the International Federation of Surveyors (FIG).

Surv. Prof. John Ayer is a Geospatialist and a Senior Lecturer at the Geomatic Engineering Department of Kwame Nkrumah University of Science and Technology. Prof. Ayer has been involved in various international and national consultancies on determination of the transformation parameters, Extending the Continental Shelf Boundary of Ghana, Liberia amongst many other geospatial areas. He has published many peer-reviewed papers in international journals. He is a Founding member and Patron of the Ghana Geospatial Society, a Member of Ghana Institution of Surveyors, Licensed Surveyors Association and the International Federation of Surveyors (FIG).

Ing. Surv. Dr. Lily Lisa Yevugah is a Geospatialist, a Lecturer and a Researcher with the Department of Geospatial Sciences. She holds PhD and MPhil degrees in Geomatic Engineering from Kwame Nkrumah University of Science and Technology in Ghana. She is a Professional Member of the Ghana Geospatial Society, Ghana Institution of Surveyors (GhIS), Ghana Institution of Engineering and the International Federation of Surveyors (FIG). Lily has been involved with research dealing with heavy metal in soils within the mining and non-mining communities as well as the application of geostatistics in the assessment and spatial mapping of pollutions across Ghana. She has also been involved in modeling and estimating carbon stocks sequestered by mangroves. Dr. Yevugah's research interests are focused mainly on applying geospatial technology in solving environmental and real-world issues such as environmental pollution, climate change, land-use change, forest management and measurement, urban sprawl, food security, natural resource management, health, etc. She is currently the Secretary of Ghana Geospatial Society.

Ing. Surv. Dr. Yaw Mensah Asare is an expert in Geomatics and a Lecturer at the Geomatic Engineering Department of the Kwame Nkrumah University of Science and Technology. Dr. Asare's research interests are focused mainly on Remote sensing and GIS application in areas such as agriculture, environmental pollution, climate change, land-use/cover change, forestry and urban environment. He also has expertise in land and hydrographic surveying. He worked as a GIS technician and a hydrographer in the underwater timber harvesting project in lake Volta, Ghana. He has ten years experience in research and higher education teaching. He has published several peer-reviewed papers in international journals. He is a Professional Member of the Ghana Geospatial Society, Ghana Institution of Surveyors, Ghana Institution of Engineering and the International Federation of Surveyors (FIG).

Contact

Name: Ing. Surv. Michael Nyoagbe

Organisation: Ghana Water Company Limited

Address: Head Office: 28th February Road (Near Independence Square) Post Office Box M 194, Accra – Ghana

Tel: +233244971602

Email: mnyoagbe@gwcl.com.gh

website: www.gwcl.com.gh